[3] M. Holm, R. Johansson, S. B. Olsson, J. Brandt, and C. Lührs, "A new method for analysis of atrial activation during chronic atrial fibrillation in man," *IEEE Trans. Biomed. Eng.*, vol. 43, pp. 198–210, Feb. 1996.
[4] J. Slocum, E. Byrom, L. McCarthy, A. Sahakian, and S. Swiryn, "Computer detection of atrioventricular dissociation from surface electrocardiograms during wide QRS complex tachycardia," *Circulation*, vol. 72, pp. 1028–1036, 1985.
[5] M. Holm, S. Pehrsson, M. Ingemansson, L. Sörnmo, R. Johansson, L. Sandhall, M. Sunemark, B. Smideberg, C. Olsson, and B. Olsson, "Non-invasive assessment of atrial refractoriness during atrial fibrillation in man—Introducing, validating and illustrating a new ECG method," *Cardiovasc. Res.*, vol. 38, pp. 69–81, 1998.
[6] S. Shkurovich, A. Sahakian, and S. Swiryn, "Detection of atrial activity from high-voltage leads of implantable ventricular defibrillators using a cancellation technique," *IEEE Trans. Biomed. Eng.*, vol. 45, pp. 229–234, Aug. 1998.
[7] N. Thakor and Y. Zhu, "Applications of adaptive filtering to ECG analysis: Noise cancellation and arrhythmia detection," *IEEE Trans. Biomed. Eng.*, vol. 38, pp. 785–793, Aug. 1991.
[8] P. Laguna, R. Jane, E. Masgrau, and P. Caminal, "The adaptive linear combiner with a periodic-impulse reference input as a linear comb filter," *Signal Proc.*, vol. 48, pp. 193–203, 1996.
[9] J. Malmivuo and R. Plonsey, *Bioelectromagnetism*. Oxford, U.K.: Oxford Univ. Press, 1995.
[10] G. J. M. Huiskamp and A. van Oosterom, "Heart position and orientation in forward and inverse electrocardiography," *Med. Biol. Eng. Comput.*, no. 30, pp. 613–620, 1992.
[11] L. Sörnmo, "Vectorcardiographic loop alignment and morphologic beat-to-beat variability," *IEEE Trans. Biomed. Eng.*, vol. 45, pp. 1401–1413, Dec. 1998.
[12] M. Åström, E. Carro, L. Sörnmo, P. Laguna, and B. Wohlfart, "Vectorcardiographic loop alignment and the measurement of morphologic beat-to-beat variability in noisy signals," *IEEE Trans. Biomed. Eng.*, vol. 46, pp. 497–506, Apr. 2000.
[13] M. Stridh, L. Sörnmo, C. Meurling, and B. Olsson, "Characterization of atrial fibrillation using the surface ECG: Spectral analysis and time-dependent properties," *IEEE Trans. Biomed. Eng.*, vol. 48, pp. 19–27, Jan. 2001.
[14] G. Golub and C. van Loan, *Matrix Computations*, 2nd ed. Baltimore, MD: The Johns Hopkins Univ. Press, 1989.
[15] M. Koschat and D. Swayne, "A weighted Procrustes criterion," *Psychometrica*, vol. 56, no. 2, pp. 229–239, 1991.
[16] L. Sörnmo, B. Wohlfart, J. Berg, and O. Pahlm, "Beat-to-beat QRS variability in the 12-lead ECG and the detection of coronary heart disease," *J. Electrocardiol.*, vol. 31, pp. 336–344, 1998.
[17] P. Young, *Electronic Communication Techniques*, 3rd ed. Columbus, OH: Merrill, 1994.
[18] E. Berbari, L. DeCarlo, B. Scherlag, and R. Lazzara, "Optimizing the signal averaging method for ventricular late potentials," in *Proc. Computers in Cardiology*, 1984, pp. 45–49.
[19] M. Stridh and L. Sörnmo. (1998) Spatiotemporal QRST cancellation techniques for atrial fibrillation analysis in the surface ECG. SPR 44 Lund Univ., Lund, Sweden. [Online]. Available: http://www.tde.lth.se/research/sig/Sigreport.html

Automatic Differentiation of Multichannel EEG Signals

B. O. Peters, G. Pfurtscheller, and H. Flyvbjerg*

***Abstract*—Intention of movement of left or right index finger, or right foot is recognized in electroencephalograms (EEGs) from three subjects. We present a multichannel classification method that uses a "committee" of artificial neural networks to do this. The classification method *automatically* finds spatial regions on the skull relevant for the classification task. Depending on subject, correct recognition of intended movement was achieved in 75%–98% of trials not seen previously by the committee, on the basis of single EEGs of one-second duration. Frequency filtering did not improve recognition. Classification was optimal during the actual movement, but a first peak in the classification success rate was observed in all subjects already when they had been cued which movement later to perform.**

***Index Terms*—Artificial neural nets, autoregressive modeling, brain-computer interface, multichannel time series analysis.**

I. Introduction

It has long been known that human electroencephalogram (EEG) activity is altered before, during, and after sensory-motor processing and other mental activities. It has also been known for some time that EEGs produced during a very limited set of mental tasks can be classified, hence recognized, according to tasks [1]–[7]. A classifier doing this can then be used to control a device by having each task correspond to a command. This concept is referred to as a *brain-computer interface* (BCI). For such applications, speed and reliability of recognition matter. A purely academical interest in the information content in EEG takes a similar interest in its dependence on the duration of the signal, circumstances of recording, and enhancement by filtering.

In this paper, we present a method that automatically finds relevant EEG channels, and classifies as well or better than other schemes. Our method was developed on data presented and studied first in [4]. These data were recorded on three subjects before, during, and after movements of right foot, left index finger, and right index finger.

Section II describes the EEG experiment. Section III describes our preprocessing, feature extraction, and classification scheme. Section IV describes our filter settings and the time course of classification of three types of movement for various frequency bands and spatial regions on the skull. In Section V, we compare our classification rates to results obtained by other groups.

II. Experimental Setup

The test subjects' EEG potentials were measured on 56 silver/silver-chloride electrodes with a reference electrode on the nose-tip. The electrodes were positioned on a rectangular grid with an approximate spacing between neighboring electrodes of 2.5 cm. Four electrodes corresponded to the international 10–20 system [8], see Fig. 1. The sampling rate, f_s, was 128 Hz, giving $56 \times 128 = 7168$

Manuscript received July 2, 1999; revised September 9, 1999. This work was supported in part by the "Fonds zur Förderung der wissenschaftlichen Forschung" in Austria under Project P11208-MED. *Asterisk indicates corresponding author.*

B. O. Peters is with the John von Neumann Institute for Computing, Forschungszentrum Jülich, D-52425 Jülich, Germany.

G. Pfurtscheller is with the Institute of Biomedical Engineering, Department of Medical Informatics, Brockmanngasse 41, A-8010 Graz, Austria.

*H. Flyvbjerg is with the Condensed Matter Physics and Chemistry Department, Risø National Laboratory, PO Box 49, DK-4000 Roskilde, Denmark, and The Niels Bohr Institute, Blegdamsvej 17, DK-2100 Copenhagen Ø, Denmark (e-mail: H.Flyvbjerg@NBI.dk).

Publisher Item Identifier S 0018-9294(01)00141-0.

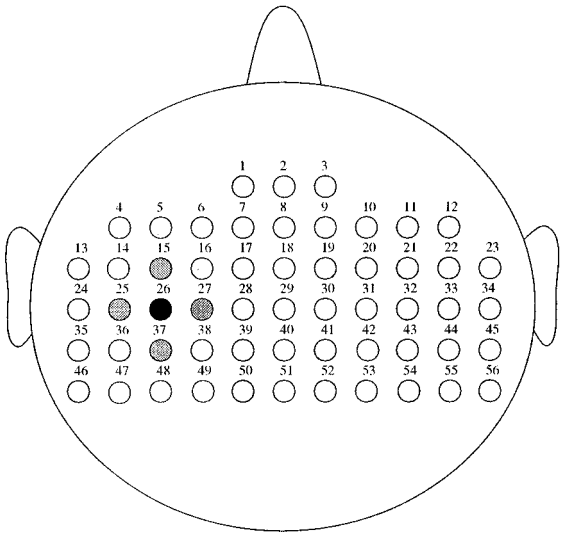

Fig. 1. Electrode positions on skull and corresponding numbering. Channel 26 corresponds approximately to position C3 in the international 10–20 system, channel 32 to C4, channel 2 to Fz, and channel 29 to Cz, respectively.

values/s to be stored. Data was recorded for at least 8 s. The EEG signals were amplified between 0.15 and 60 Hz (3 dB points, 16 dB/octave) with two coupled 32-channel amplifier systems (BEST, Fa. Grossegger, Austria).

The experimental protocol used to obtain these EEGs is as follows: Two seconds after recording was begun, the subject was alerted by a short beep [*warning stimulus* (WS)]. One second after the beep, an arrow pointing left, right, up, or down appeared on a screen for 300 ms, indicating that the left (left arrow) or right index finger (right), the right foot (down), or the tongue (up) soon was to be moved (CUE). Data recorded for tongue movement were mostly corrupted by electrical signals from the movement itself, and were excluded from further analysis. The remaining three events we refer to as L, R, and F, respectively. The subject had been instructed to move the relevant extremity in a brisk movement, but only some time *after* a second acoustic *reaction stimulus* (RS) had sounded at 5 s [4]. The time between RS and onset of movement was 0.5 to 1.5 s.

In this way, 37–77 trials were recorded for each of L, R, and F from three subjects, referred to as A4, B6, and B8 below (cf. Table I). The subjects were all healthy, right-handed students, aged 23–29, two male (A4 and B8) and one female (B6).

III. Signal Processing

A. Autoregressive Models and Feature Vector Extraction

We use standard autoregressive (AR) models as power spectrum estimators, and use their coefficients as feature vectors: Each EEG-channel's signal $x(t)$ at time t is estimated by a linear combination of its values at the p former instants, $\hat{x}(t) = \sum_{k=1}^{p} a_k^p x(t-k\cdot\Delta t)$, where $\Delta t = 1/f_s$ is the sampling time and p is the AR model order. The AR coefficients, $(a_k^p)_{k=1\ldots p}$, are obtained by minimizing the squared error $\sum_t \{e(t)\}^2 = \sum_t \{\hat{x}(t) - x(t)\}^2$. The difference $e(t) = x(t) - \hat{x}(t)$ is assumed to be white noise with variance σ^2. Consequently, the power spectrum is estimated by

$$|\tilde{X}_{\mathrm{AR}}(f)|^2 = \frac{\sigma^2}{\left|1 - \sum_{k=1}^{p} a_k^p \cdot e^{-i2\pi(f/f_s)\cdot k}\right|^2}$$

TABLE I
Number of Trials Recorded for Each Subject and Each Event

subject	L	R	F	sum
A4	73	73	77	223
B6	55	54	64	173
B8	37	48	39	124

and the AR coefficients, $(a_k^p)_{k=1\ldots p}$, are used as *feature vector*, representing the data in this one channel during a time interval of 1 or 0.5 s during one trial.

The optimal AR model order, p, can be determined by information theoretic methods [9]. The classification result of our classifier is already an information measure, however. Thus, the optimal value for p is the one yielding maximal classification success, once that has been defined.

B. Artificial Neural Network as classifier

An artificial neural network (ANN) is a general-purpose function approximator for multidimensional functions of several variables [10]. We used an ANN consisting of three perceptrons, one perceptron for each of the classes L, R, and F. (Initially, we used ANNs with one hidden layer, but an investigation of their weights after training indicated that the simpler perceptrons would be as efficient, and they actually were better [11]. This indicates that simpler, purely linear schemes may work as well, e.g., independent component analysis [12].) The p-dimensional feature vectors were used as input variables. The output of a perceptron was supposed to be positive if a feature vector at its input encoded the movement that the perceptron classified for, and negative if it did not. An output value close to zero indicated that the perceptron did not have much of an "opinion," while a numerically larger output indicated a stronger opinion.

The gradient descent method [10] was used to train the ANN on a subset of all feature vectors, the *training set*. The ability of the ANN to correctly classify feature vectors was monitored on a second, independent subset of trials, the *validation set*. As training proceeded, the classification success on the validation set first increased, but eventually decreased when the ANN started over-learning [10]. We stopped training when the classification success on the validation set had reached its maximum, in order to ensure the ANNs generalization ability.

The ANNs success on the validation set does not represent its true generalization ability. The latter is lower because the validation set was used for optimization. Consequently, we used a third, independent, *test set* on which we evaluate the classifier's success rate. The partitioning of the available experimental trials on training, validation, and test sets was done at random. The training set and the validation set must both consist of an equal number of trials from classes L, R, and F. Otherwise, the classifier will be biased toward the class from which it has seen most feature vectors. For subject A4, e.g., we used $50+50+50$ trials in the training set, $16+16+16$ trials in the validation set, and $7+7+11$ trials in the test set, for each of the classes L, R and F, respectively.

C. Multichannel Signal Processing: The "Committee" Method

For each individual channel in the EEG, an ANN was trained as just described. Each ANN gave a three-dimensional output vector with its "opinion" about a given input. These output vectors were summed up, and the sum was used to classify the input, according to which component in the output vector sum was largest, i.e., "received the strongest vote."

This procedure was based on the observation that perceptrons with a "strong conviction" (large output value) tended to be right, while perceptrons with a weak conviction (output near zero) more often were wrong. Thus, by weighting an opinion by its strength, the emphasis is

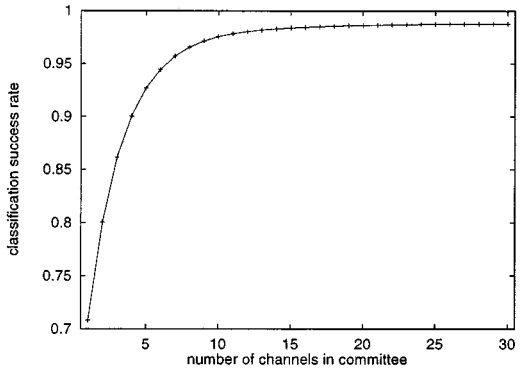

Fig. 2. Classification success averaged over trials from the validation set as function of committee size. The results shown were obtained by averaging over 5000 random partitions of available trials in training, validation, and test set. Laplace filtered data (Section III-D1) from subject A4 were used, analyzed as AR(10) coefficients computed in the period from 5 to 6 s. No bandpass filter (Section III-D2) was applied.

placed on opinions that are correct with a high probability, while opinions that are less probably correct are de-emphasised and left to cancel each other. Since the latter's contribution mainly is noise, we consequently left the decision to a committee that excluded them, as follows.

According to the classification success on the trials in the validation set, the 30 channels were rank-ordered. N-member "committees" were formed from the N ANNs with the best classification success, with N ranging from one to 30. The classification success rate, averaged over the trials in the validation set, was computed as a function of the committee size N. Fig. 2 shows this function.

The committees' classification accuracy depends on N, the number of committee members. The accuracy rises first quickly with increasing N, then very slowly for $N > 10$. The average classification success does not vary significantly for committee sizes bigger than 15: The channels above this size do not contribute any additional information. Hence, we decided to use a committee of size $N = 20$.

With the committee size and the corresponding member-ANNs chosen, our design procedure for a classifier is complete (for given pre-processing; see following section): We have a particular set of channels with associated trained ANNs, and a rule for how to combine and interpret the outputs of these ANNs. The predictive power of this committee is then tested on the trials in the test set.

The whole procedure just described was repeated 100 to 500 times, each time partitioning the set of trials in a random manner on training, validation, and test set, and each time initiating each ANN with new random weights before training.

The committee yielded better classification accuracy than any individual channel could provide, and is a way to combine information from several channels, i.e., from different spatial regions. Thus, a nontrivial task is solved, that of choosing optimal electrode positions and the optimal number of channels for an EEG-based brain-state classifier. In the literature, the choice of EEG channels for this purpose is done either by hand, by competent physiologists, or in preliminary studies [13].

D. Preprocessing and Parameter Settings

Before the power spectra are modeled with AR models, some preprocessing is necessary to obtain an optimal result. Ideally, the preprocessing scheme should be tailored to the individual subject, if the goal is an optimized BCI for a given subject. Since this is computationally difficult, we did this only for one subject, A4. We changed the algorithmic parameters only one by one, keeping the others constant, while monitoring our scheme's classification success. For this reason, and

TABLE II
THREE-STATES CLASSIFICATION RESULTS OBTAINED WITH VARIOUS SPATIAL AND FREQUENCY FILTER SETTINGS FOR SUBJECT A4

subject A4	spatial filters			
band pass	CAR	Laplace	LAT	none
0–6 Hz	97	96	78	84
8–12 Hz	97	97	77	83
19–26 Hz	97	97	83	87
38–42 Hz	92	96	77	81
none	98	98	84	87

EEG data were extracted in the period of the onset of movement, between 5 and 6 s. Classification was done on coefficients of AR (10) models fitted to data in each channel. Results given are percent of trials in the test set correctly classified by the committee. Differences of more than 2% are statistically significant.

because we only study three subjects in total, our results should not be considered conclusive. More subjects need to be studied, in a more general search for optimal parameter settings. For now, we observe that such a wider search for optimal performance only can yield higher success rates than those obtained here, everything equal and assuming our three subjects typical.

1) Spatial Filtering: The 56 channels do not provide independent information. We computed the correlations between channels in subject A4's EEG, and found channels as far as 15 cm apart were 60%–70% correlated. Spatial filtering can remove much of this correlation. With the notation $x_k(t)$ for the signal in channel k, the spatial filters considered were *common average reference*, or CAR ($x'_k(t) = x_k(t) - (1/56)\sum_{i=1}^{56} x_i(t)$), and *Laplace filter* ($x'_{26} = x_{26} - (1/4)\{x_{15} + x_{25} + x_{27} + x_{37}\}$). In addition, we studied a *local average technique*, or LAT (e.g., $x'_{26} = (1/5)\{x_{15} + x_{25} + x_{26} + x_{27} + x_{37}\}$),

Both CAR and Laplace filtering remove the influence of the reference electrode. Laplace filtering additionally removes any linear spatial component, and has hence some high-pass filter characteristics. On the other hand, LAT introduces a spatial low-pass filter. For both LAT and Laplace filter, only the 30 electrodes with four nearest neighbors could be analyzed, of course.

2) Frequency Filtering: Even before actual movement, EEG activity in characteristic regions are synchronised or desynchronised in specific frequency bands [14]–[16]. Low and high frequency activity in surface EEGs is not related to movement [17]. We used a causal Kaiser filter of length $N_K = 25$ ($\approx$200 ms at our $f_s = 128$ Hz) and Kaiser parameter $\alpha_K = 2$ [18]. We filtered the data in the *theta* (0–6 Hz), the *alpha* (8–12 Hz), the *beta* (19–26 Hz), and the *gamma* (38–42 Hz) frequency band.

IV. RESULTS

A. AR Model Order and Filter Settings

We measured the classification success rate of subject A4, on Laplace filtered segments of EEG data taken in the period from 5 to 6 s. The classification was done on the coefficients of AR (p) models, with p varying from two to 50. The classification success rate increased with p until $p \approx 10$, then stayed at approximately the same level until $p \approx 20$, and decreased slowly for larger values of p. We consequently chose $p = 10$. This procedure relied on brute force, of which we had plenty, and is intellectually economical by its directness.

To study the influence of spatial and bandpass filters, we classified EEG data from subject A4 in the time interval between 5 and 6 s, i.e., before the onset of movements in most trials. The lower right entry in Table II shows that raw data already yield 87% success. The last column in Table II shows that bandpass filtering does not improve the success rate.

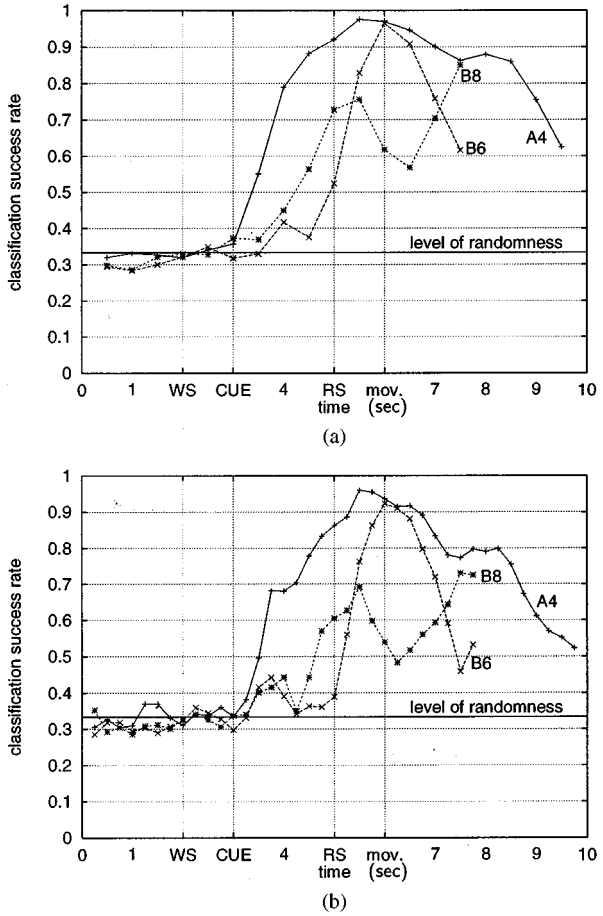

Fig. 3. Classification results as function of time for subjects A4, B6, and B8. Success rate 1 represents perfect recognition. Random guessing would result in success rate $1/3$. (a) Classification based on 1 s-intervals. (b) Classification based on 500-ms intervals. The plotting symbols are located in the middle of the corresponding time intervals. Results shown are averages of 500 partitionings of the trials on training, validation, and test set.

Of the spatial filtering techniques, LAT was worse than no filter. CAR and Laplace filters work equally well in the absense of bandpass filters, yielding 98% success. We chose the Laplace filter because it works equally well with all bandpass filters. But we might as well have chosen CAR, because we chose to use no bandpass filter. All results reported below were obtained with this choice.

B. Error Reduction

In order to reduce fluctuations due to finite statistics, the random partitioning of trials on training, validation, and test sets was repeated at least 100 times, and performance results were averaged [19]. This procedure reduced the standard error on our rates by a factor two, approximately. This we found by applying the method to synthetic data sets with known properties. The resulting standard error of approximately 5% compares well with the fluctuations around the value $1/3$ seen in the recognition rates before the cue at 3 s in Figs. 3 and 4.

C. Time Course of Classification

The classifier's performance on the EEG signal is shown as a function of time in Fig. 3. Before the subjects have been told which movement to perform, the success rate corresponds to random guessing, as it should. Immediately after they have been told, but before the actual

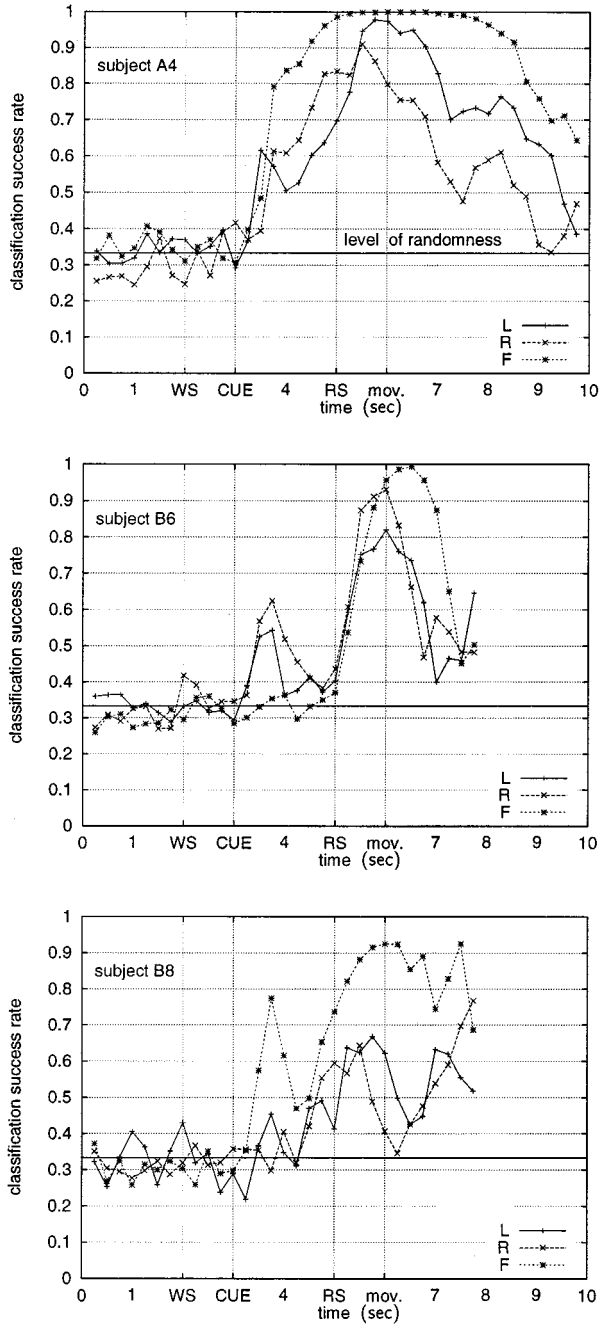

Fig. 4. Classification success rates for individual events: left finger (L), right finger (R), and right foot (F), for subjects A4, B6, and B8. Rates shown are the number of correctly recognized trials of event X divided by the number of trials of event X in the test set.

movement, the success rate grows. It peaks at the time of the actual movement, and it is high even 2–3 s *after*.

Fig. 3(b) has twice the time resolution of Fig. 3(a) and reveals more structure in the EEG. Success rates in Fig. 3(b) are slightly lower than in Fig. 3(a) because the EEG signals used last half as long. But in the time window 500 ms after the visual cue was presented, the rates briefly reach a maximum for all subjects. For subject A4 the rate remains near 70% until just before RS, while for subjects B6 and B8 the rate quickly drops to the randomness level, then grows to a higher maximum at the time of the actual movement. For subject B8 there is a third, higher maximum in the classification success rate near the end of the EEG recording period. This increased classification rate in subject B8 after

movement-offset may be explained by the post-movement beta synchronization localized close to the corresponding primary motor area [20]–[22].

D. Classification Accuracy for Individual Movements

Fig. 4 shows the classification success rates for the individual events. We note that these rates differ a good deal from each other and between subjects. A4 and B8 have some properties in common: Recognition of foot movement (F) and intention of foot movement is higher than L and R recognition; recognition of R is higher than L before the movement, but lower than L after the movement. Fig. 4 also reveals that the peak in Fig. 3 immediately after the CUE is caused by different events for the three subjects. Finally, in all subjects the classification of L and R decreases after the movement, then increases again after approximately 7 s recording time.

E. Spatial Analysis

The electrodes chosen for the committee were mostly grouped around the electrode positions C3 and C4 (cf. Fig. 1), i.e., above the motor cortex. There were, however, considerable intersubject differences. For subject A4, the spatial regions of good recognition remained the same during the time from 3.5 to 8 s; the central region of the skull did not play an important role in the classification task. In subject B6, there was a peak at the frontal and central electrodes during the time period of early classification (3.5–4 s) which vanished during the movement. The electrodes situated frontally and parietally from the positions C3 and C4 are those included most often in the committee. In subject B8, the first peak of classification at time 3.5–4 s (cf. Fig. 3) goes out from right regions of the skull, a phenomenon which can be explained by the higher L, contralateral, recognition at this time (cf. Fig. 4).

V. Discussion

In this section, we compare our results with other published results obtained with the same subjects. Because of the high intersubject variability of EEGs, this comparison provides the best possible test of our classification method against other methods. We also compare our results with results from different experiments: The subjects providing the data analyzed above have participated in earlier experiments [13] with a slightly different experimental paradigm: Between the visual cue on the screen and the reaction stimulus, there was only one second instead of two, and the average time between reaction stimulus and onset of movement was 500 ms instead of the 1000 ms in our study. Classification was done on up to 56 EEG channels, using the ERD or ERS in specific frequency bands as features. The classifier was a so-called *distinction sensitive learning vector quantiser* (DSLVQ) [23].

The *best* results for the classification of left and right index finger movements reported in [13] were as follows.

Subject A4: all 56 electrodes, power in the 10–12 Hz frequency band: $79.3 \pm 2.5\%$;

Subject B6: 11 electrodes pre-selected on the same data set by a preliminary experiment, power in the 20–24 Hz frequency band: $88.6 \pm 1.2\%$;

Subject B8: 11 electrodes preselected by an expert, frequency band 10–12 Hz: $84.5 \pm 2.2\%$.

In [4], classification success rates up to 89% were reported for left/right index finger movement discrimination for a subject whose records in earlier experiments had shown significant changes in 40-Hz EEG during finger movement.

Our classification results were obtained for the same subjects as studied in [13]. When we applied our classifier to mere left/right index finger discrimination, we found succes rates of 94% for subject A4, 95% for subject B6, and 91% for subject B8, for EEGs measured in the time interval between 5 and 6 s recording time.

In another experiment investigating the possibility of a BCI, the ERD was used to classify three types of movement (L, R, and F) in four subjects, including subject B8 of our study [7]. After a short WS, a visual cue was presented to the subjects for 1.25 s, during which ERD patterns in narrow frequency bands were extracted from channels C_3, C_z, and C_4. After the visual cue had vanished, the corresponding L, R, or F movement had to be performed. Approximately one second later, the estimate of the DSLVQ classifier was fed back to the subject. The classification result for the three movements of that study reached 50%–70% after several sessions.

With our method, we obtained 98% correct classification of the three events for subject A4, a maximum of 96% for subject B6, and 75% correct recognition for subject B8 before movement, and even 85% in the interval from 7 to 8 s, see Fig. 3.

Our results raise hope that it may be possible in general to classify EEGs according to tasks with quite high accuracy. The data, however, were taken from subjects who were prompted to specific tasks by a computer. With a BCI, one wants the subject to prompt the computer to specific tasks. Thus, further progress toward a BCI requires data from experiments where the *subjects* decide which "brain state" to produce, e.g., by thinking about a movement as if intending to perform it. In such experiments, the classification results could with advantage be fed back to the subject, as Wolpaw and McFarland do [2], to help the subject learn to produce a small "dictionary" of distinguishable EEG patterns. But as the subject through feedback optimizes his performance with the classifier, the classifier should also be reoptimized every so often, it should be "retrained" to the subject's changed EEGs, and the change in classifier will provide a measure of the change in the EEGs, including the change in their information content. The classifier presented here is convenient for this purpose, since retraining can be done automatically whenever desired, as long as EEGs have been recorded for the purpose.

Acknowledgment

The authors thank W. Bialek, P. Grassberger, and J. Müller-Gerking for fruitful discussions. B. O. Peters thanks the Zentralinstitut für Angewandte Mathematik, Jülich, for generous allocation of Cray T3E time and technical support, and the Danish Research Academy's *Graduate School of Biophysics* for hospitality while finishing this article.

References

[1] Z. A. Keirn and J. I. Aunon, "A new mode of communication between man and his surroundings," *IEEE Trans. Biomed. Eng.*, vol. 37, pp. 1209–1214, 1990.

[2] J. R. Wolpaw and D. J. McFarland, "Multichannel EEG-based brain-computer communication," *Electroenceph. Clin. Neurophysiol.*, vol. 90, pp. 444–449, 1994.

[3] M. Peltoranta and G. Pfurtscheller, "Neural network based classification of nonaveraged event-related EEG responses," *Med. Biol. Eng. Computing*, vol. 32, pp. 189–196, 1994.

[4] G. Pfurtscheller, D. Flotzinger, and C. Neuper, "Differentiation between finger, toe and tongue movement in man based on 40 Hz EEG," *Electroenceph. Clin. Neurophysiol.*, vol. 90, pp. 456–460, 1994.

[5] C. W. Anderson, S. Devulapalli, and E. A. Stolz, "Determining mental states from EEG signals using parallel implementations of neural networks," *Scientific Programming*, vol. 4, pp. 171–183, 1995.

[6] C. W. Anderson, "Effects of variations in neural network topology and output averaging on the discrimination of mental tasks from spontaneous electroencephalogram," *J. Intelligent Syst.*, vol. 7, pp. 165–190, 1997.

[7] J. Kalcher, D. Flotzinger, C. Neuper, S. Gölly, and G. Pfurtscheller, "Graz brain-computer interface II: Toward communication between humans and computers based on online classification of three different EEG patterns," *Med. Biol. Eng. Computing*, vol. 34, pp. 382–388, 1996.

[8] H. Jasper, "The ten-twenty electrode system of the international federation," *Electroenceph. Clin. Neurophysiol.*, vol. 10, pp. 371–375, 1958.

[9] D. G. Childers, *Modern Spectrum Analysis*. Piscataway, NJ: IEEE Press, 1978.
[10] J. Hertz, A. Krogh, and R. G. Palmer, *Introduction to the Theory of Neural Computation*. San Francisco, CA: Addison-Wesley, 1991.
[11] B. O. Peters, G. Pfurtscheller, and H. Flyvbjerg, "Prompt recognition of brain states by their EEG signals," *Theory Biosci.*, vol. 116, pp. 247–258, 1997.
[12] J. Müller-Gerking, G. Pfurtscheller, and H. Flyvbjerg, "Designing optimal spatial filters for single-trial EEG classification in a movement task," *Clin. Neurophysiol.*, vol. 110, pp. 787–798, 1999.
[13] M. Pregenzer, G. Pfurtscheller, and D. Flotzinger, "Selection of electrode positions for an EEG-based brain computer interface (BCI)," *Biomedizinische Technik*, vol. 39, pp. 264–269, 1994.
[14] G. Pfurtscheller and A. Aranibar, "Event-related cortical desynchronization detected by power measurement of scalp EEG," *Electroenceph. Clin. Neurophysiol.*, vol. 42, pp. 817–826, 1977.
[15] ——, "Evaluation of event-related desynchronization (ERD) preceding and following voluntary self-paced movement," *Electroenceph. Clin. Neurophysiol.*, vol. 46, pp. 138–146, 1979.
[16] G. Pfurtscheller and C. Neuper, "Event-related synchronization of mu rhythm in the EEG over the cortical area in man," *Neurosci. Lett.*, vol. 174, pp. 93–96, 1994.
[17] P. L. Nunez and R. Katznelson, *Electrical Fields of the Brain—The Neurophysics of EEG*. New York: Oxford Univ., 1981.
[18] J. R. Johnson, *Introduction to Digital Signal Processing*, London, U.K.: Prentice-Hall, 1991.
[19] B. Efron and R. J. Tibshirani, *An Introduction to the Bootstrap*, London, U.K.: Chapman & Hall, 1993.
[20] C. Toro, G. Deuschl, R. Thatcher, S. Sato, C. Kufta, and M. Hallett, "Event-related desynchronization and movement-related cortical potentials on the ECoG and EEG," *Electroenceph. Clin. Neurophysiol.*, vol. 93, pp. 380–389, 1994.
[21] C. Neuper and G. Pfurtscheller, "Post-movement synchronization of beta rhythms in EEG over the cortical foot area in man," *Neurosci. Lett.*, vol. 216, pp. 17–20, 1996.
[22] G. Pfurtscheller, A. Stancák Jr., and G. Edlinger, "On the existence of different types of central beta rhythms below 30 Hz," *Electroenceph. Clin. Neurophysiol.*, vol. 102, pp. 316–325, 1997.
[23] M. Pregenzer, D. Flotzinger, and G. Pfurtscheller, "Distinction sensitive learning vector quantizer—A noise-insensitive classification method," in *Proc.ICNN-94*, Orlando, FL, 1994, pp. 2890–2894.

Strain Imaging and Elasticity Reconstruction of Arteries Based on Intravascular Ultrasound Video Images

Mingxi Wan*, Yangmei Li, Junbo Li, *Student Member, IEEE*, Yaoyao Cui, and Xiaodong Zhou

***Abstract*—Based on intravascular ultrasound (IVUS) video images, a novel motion estimation method combining the genetic algorithm-based optical flow method and a step-by-step and sum strategy has been developed to estimate the displacement and strain distributions on the scan cross sections of the arteries. And then, real elasticity distributions were reconstructed under the conditions of small and large deformation. Experimental results of *in vitro* porcine arteries demonstrated the feasibility of the method. This investigation may have potentials to provide new technological means for monitoring and evaluating percutaneous transluminal coronary angioplasty procedure, especially, for the end users of IVUSpercimaging equipment.**

***Index Terms*—Elasticity reconstruction, *in vitro* porcine artery, intravascular ultrasound, strain imaging, video echo image.**

I. Introduction

Percutaneous transluminal coronary angioplasty (PTCA), during which a small balloon is inserted into a partially occluded coronary artery and pressurized with fluid to expand the vessel, is evolving into one of the accepted most common therapeutic procedures for atherosclerotic coronary diseases [1]. However, the plaques in the artery with different elasticity moduli respond differently to the PTCA procedure. Furthermore, the appraisement of the PTCA procedure depends on the morphological and mechanical properties of the treated plaques and artery tissues. Therefore, the acquisition of the artery elasticity with submillimeter resolution is of great importance during PTCA procedure.

Several groups are now investigating in feasibility of intravascular ultrasound (IVUS) elasticity imaging. De Korte *et al.* [2] developed a technique for obtaining the local strains of the vessel-like phantoms. Time shifts between radio frequency (RF) gated echoes acquired at two levels of intravascular pressures were estimated using one-dimensional correlation with bandlimited interpolation around the correlation peaks. Shapo *et al.* [3] employed a correlation-based phase-sensitive speckle tracking algorithm acted on RF echoes to compute strains of a cylindrical homogeneous phantom and generate radial strain profiles. Talhami *et al.* [4] described a spectral process on IVUS echoes to compute the average radial strains for the entire vessel wall thickness at each angular position of the scan beam, which were displayed as a color-coded ring overlaid on conventional IVUS image. This method is based on the Fourier scaling property of IVUS RF echoes and the change of the mean scatterer spacing that resulted from vessel wall compression. Ryan *et al.* [5] used a two-dimensional (2-D) correlation speckle tracking algorithm acted on serial intravascular

Manuscript received March 1, 1999; revised September 6, 2000. This work was supported by National Natural Science Foundation of China under Grants 39970208, 69925101 and by the Chinese government under the Trans-century Training Program Foundation for Talent. *Asterisk indicates corresponding author.*

*M. Wan is with the Department of Biomedical Engineering, Xi'an Jiaotong University, Xi'an, 710049, China (e-mail: mxwan@xjtu.edu.cn).

Y. Li, J. Li, and Y. Cui are with the Department of Biomedical Engineering, Xi'an Jiaotong University, Xi'an, 710049, China.

X. Zhou is with the Department of Medical Ultrasound at the Xijing Hospital and the Fourth Military Medical University, Xi'an, 710032, China.

Publisher Item Identifier S 0018-9294(01)00142-2.